



Inversion of Asymmetric Vortex Vein Dilatation in Pachychoroid Spectrum Diseases

Hidetaka Matsumoto, MD, PhD, Shoji Kishi, MD, PhD, Junki Hoshino, MD, Kosuke Nakamura, MD, Hideo Akiyama, MD, PhD

Purpose: Intervortex venous anastomosis is widely recognized as compensating for vortex vein congestion in pachychoroid spectrum diseases. However, determining the blood flow direction within the compensated drainage route is often challenging. Herein, we investigated the morphological patterns of vortex veins in eyes showing retrograde pulsatile vortex venous flow.

Design: Retrospective observational case series.

Subjects: Six hundred eighty-nine consecutive eyes with treatment-naïve central serous chorioretinopathy, pachychoroid neovascularopathy, or polypoidal choroidal vasculopathy.

Methods: We reviewed the clinical records of patients with these pachychoroid spectrum diseases. Multimodal images including indocyanine green angiography (ICGA) and en face OCT were analyzed.

Main Outcome Measures: Intervortex venous anastomosis between superotemporal and inferotemporal vortex veins and the dominant site of dilated temporal vortex veins were determined in the eyes with retrograde pulsatile vortex venous flow in the temporal vortex veins.

Results: Twenty-two eyes with retrograde pulsatile vortex venous flow in the temporal vortex veins were identified utilizing early phase ICGA videos. In 9 eyes, retrograde pulsatile flow was detected in the superotemporal vortex veins, which were connected to the inferotemporal vortex veins via intervortex venous anastomoses. Among these cases, contralateral inferotemporal vortex vein dilatation was dominant in 7 eyes (77.8%), while superotemporal and inferotemporal vortex veins were symmetrically dilated in the other 2 eyes (22.2%). On the other hand, in 13 eyes, the retrograde pulsatile flow was detected in the inferotemporal vortex veins, which were linked to the superotemporal vortex veins via intervortex venous anastomoses. In these eyes, contralateral superotemporal vortex vein dilatation was dominant in 10 eyes (76.9%). Superotemporal and inferotemporal vortex veins were symmetrically dilated in 2 eyes (15.4%), while mainly inferotemporal vortex veins were dilated in 1 eye (7.7%).

Conclusions: In pachychoroid spectrum diseases, there are cases wherein congested venous blood might drain into the contralateral vortex veins via intervortex anastomoses. Overloaded contralateral vortex veins may, as a consequence, become more dilated than the primary congested vortex veins. Inversion of asymmetric vortex vein dilatation might thereby develop in pachychoroid spectrum diseases.

Financial Disclosure(s): Proprietary or commercial disclosure may be found in the Footnotes and Disclosures at the end of this article. *Ophthalmology Science* 2024;4:100515 © 2024 by the American Academy of Ophthalmology. This is an open access article under the CC BY-NC-ND license (<http://creativecommons.org/licenses/by-nc-nd/4.0/>).



Supplemental material available at www.ophtalmologyscience.org.

Freund et al were the first to use the term “pachychoroid” to describe choroidal thickening associated with dilatation of outer choroidal vessels.¹ The pachychoroid concept has facilitated clinicians’ understanding of pachychoroid spectrum diseases including central serous chorioretinopathy (CSC), pachychoroid pigment epitheliopathy, pachychoroid neovascularopathy (PNV), and polypoidal choroidal vasculopathy (PCV).^{2,3} Moreover, recent studies have suggested that pachychoroid might be involved in the development of age-related macular

degeneration in Asian populations.^{4,5} Although the diagnostic criteria for pachychoroid have not as yet been established, characteristic features of pachychoroid including pathological dilatation of vortex veins have been reported.^{1–3} The pathogenesis of pachychoroid also has not been fully elucidated, although previous studies have suggested the involvement of vortex vein congestion, in other words, choroidal venous overload.^{6,7}

Pang et al reported dilated vortex veins from the ampulla to the posterior pole in CSC employing ultrawidefield

indocyanine green angiography (ICGA).⁸ Hiroe and Kishi documented asymmetric dilatation of superotemporal and inferotemporal vortex veins in CSC utilizing en face OCT.⁹ We demonstrated the area of choriocapillaris filling delay on ICGA to frequently overlap with that of dilated vortex veins detected by en face OCT in eyes with CSC or PNV.^{10,11} We also found the horizontal watershed zone to be lost due to anastomoses between the superotemporal and inferotemporal vortex veins in over 90% of reported cases with CSC, PNV, or PCV.^{12–14} Based on our use of the early phase of video ICGA, we previously reported pulsatile flow in vortex veins connected to the anastomotic vessels between the superior and inferior vortex veins in 25.8% of eyes with these pachychoroid spectrum diseases.¹⁵ Although determining pulsatile flow direction is often challenging, retrograde pulsatile flow was detected in 18.4% of our previously reported cases with pulsatile vortex venous flow.¹⁵ Taken together, these clinical findings indicate vortex vein congestion to possibly be involved in the pathogenesis of pachychoroid spectrum diseases. Based on these results, we developed a monkey model of vortex vein congestion by ligating the vortex veins on the scleral surface.¹⁶ This monkey model showed vortex vein dilatation, choroidal thickening, intervortex venous anastomosis, choriocapillaris filling delay, and pulsatile vortex venous flow, as observed in pachychoroid spectrum diseases. Therefore, our novel animal model supports the hypothesis that vortex vein congestion is involved in the pathogenesis of pachychoroid.

Vortex venous blood normally flows from the posterior pole to the vortex vein ampullas, centrifugally, and then drains out of the eye through the sclera.¹⁷ When vortex venous blood flow becomes congested, the vortex veins are thought to become dilated due to the increased venous pressure. Numerous reports have described the morphological features of vortex veins in pachychoroid spectrum diseases, based on OCT and ICGA findings. However, few studies have examined the relationship between the direction of blood flow in vortex veins and the morphological characteristics of these vessels.^{15,18} In the present study, we evaluated the morphological features of vortex veins in eyes with pachychoroid spectrum diseases showing retrograde pulsatile vortex venous flow on ICGA. Next, we explored the potential for remodeling of the venous drainage route in eyes with these diseases.

Methods

This study, which complied with the guidelines of the Declaration of Helsinki, was performed with approval from the Institutional Review Board of Gunma University Hospital. An opt-out informed consent protocol was used for this study. We retrospectively studied 689 eyes of 681 patients with treatment-naïve pachychoroid spectrum diseases including 271 eyes with CSC, 196 with PNV, and 222 with PCV, followed clinically from April 2017 through November 2023 at Gunma University Hospital.

All patients underwent a complete ophthalmological examination, including color fundus photography (Canon CX-1; Canon Inc), swept-source OCT (DRI OCT-1 Triton; Topcon Corp, and

Table 1. Demographic and Clinical Characteristics of Patients with Pachychoroid Spectrum Diseases Showing Retrograde Pulsatile Vortex Venous Flow

Number of Eyes	22
Number of patients	22
Age (years)	71.4 ± 9.8
Male	20 (90.9%)
Disease type	
CSC	5 (22.7%)
PNV	11 (50.0%)
PCV	6 (27.3%)
Central choroidal thickness (µm)	285 ± 83
Retrograde flow in superotemporal vortex veins	9
Dominant site of vortex vein dilatation	
Superotemporal	0 (0.0%)
Symmetric	2 (22.2%)
Inferotemporal	7 (77.8%)
Retrograde flow in inferotemporal vortex veins	13
Dominant site of vortex vein dilatation	
Superotemporal	10 (76.9%)
Symmetric	2 (15.4%)
Inferotemporal	1 (7.7%)

CSC = central serous chorioretinopathy; PCV = polypoidal choroidal vasculopathy; PNV = pachychoroid neovasculopathy.

PLEX Elite 9000; Carl Zeiss Meditec), as well as both fluorescein angiography (FA) and ICGA (Spectralis HRA + OCT; Heidelberg Engineering). We obtained B-mode images of the horizontal and vertical line scans (12 mm) through the fovea as well as 12 radial scans (9 mm) centered on the fovea employing the DRI OCT-1 Triton. Next, cube data were acquired with a raster scan protocol of 1024 (horizontal) × 1024 (vertical) B-scans, which covered the 12 × 12 mm area centered on the fovea, employing the PLEX Elite 9000. En face images were obtained from the vitreous to the choroidoscleral border with coronal slices from a 3-dimensional dataset included in the inner software. Then, we performed optical coherence tomography angiography (OCTA) volume scanning, i.e., 300 × 300 pixels in the 3 × 3 mm area demonstrated by the PLEX Elite 9000. The OCTA was based on an optical microangiography algorithm. For the ICGA examinations, we injected 25 mg/2 ml of indocyanine green solution into the medial cubital vein of the right arm in all patients. We recorded the video-ICGA centered on the fovea with an angle of 30° for the first 30 seconds after choroidal filling. Then, we obtained widefield ICGA images centered on the fovea with an angle of 102°. For the cases evaluated after June 2019, we additionally conducted ultrawidefield ICGA (California; Optos). Moreover, in the cases assessed after December 2021, we acquired 3-dimensional volume data of vertical 20 mm (1024 B-scans) × horizontal 23 mm (1024 pixels) scans, also centered on the fovea, employing enhanced depth imaging of swept-source OCT (Xephilio OCT-S1; Canon Inc.). Built-in software supported by artificial intelligence was used to automatically segment the total choroid. Widefield en face OCT images of the choroid were then generated.

For this study, clinical and anatomical features of the pachychoroid were defined as pathologically dilated outer choroidal vessels accompanied by thinning of Sattler's layer and the choriocapillaris on B-mode and en face OCT as well as ICGA images. Central choroidal thickness (CCT) was not included among the pachychoroid criteria applied because CCT is influenced by both age and refractive errors.¹⁹ Furthermore, eyes with

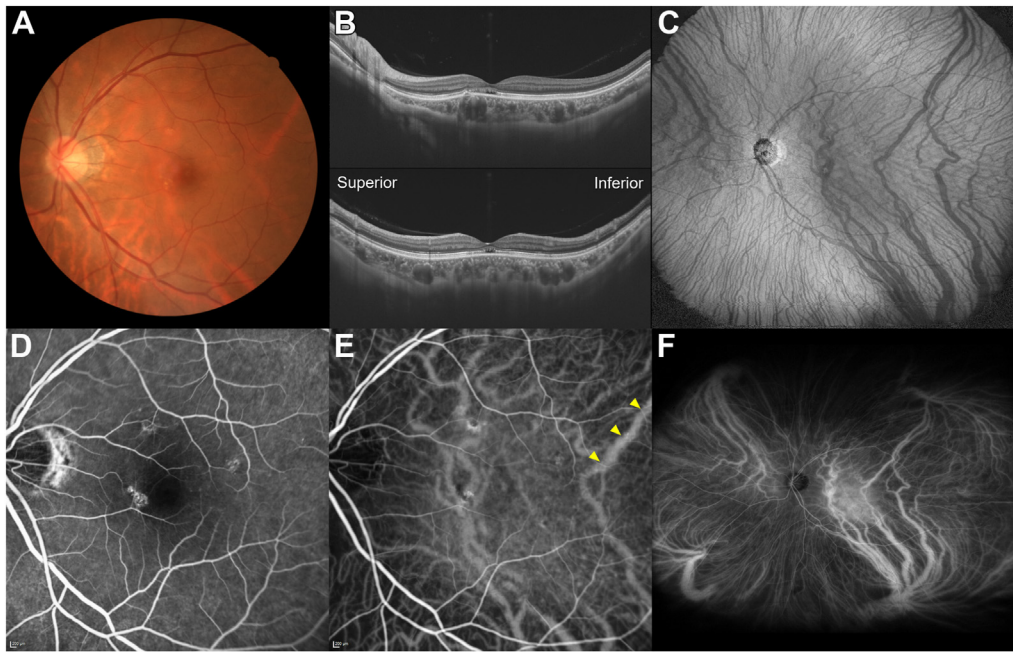


Figure 1. Images of the left eye of a 57-year-old woman with central serous chorioretinopathy. Best-corrected visual acuity was 0.52 logarithm of the minimum angle of resolution unit. **A**, Color fundus photograph shows retinal pigment epithelium (RPE) abnormality nasal to the fovea. **B**, Twelve-millimeter horizontal and vertical B-mode OCT images through the fovea show pachychoroid with dilated outer choroidal vessels (vortex veins). A small RPE detachment accompanied by subretinal fluid is observed at the macula. The central choroidal thickness is 334 μm . **C**, En face OCT image (20 mm \times 23 mm) of the choroid shows dilated vortex veins. The horizontal watershed has been lost due to anastomoses between the superotemporal and inferotemporal vortex veins. Inferotemporal vortex veins are more dilated than superotemporal vortex veins. **D**, Fluorescein angiography shows window defects and mild leakage nasal to the fovea. **E**, Indocyanine green angiography (ICGA) shows anastomotic dilated vortex veins. Retrograde pulsatile flow is detected in the superotemporal vortex veins (arrowheads). Venous blood flows from superotemporal vortex veins affected by primary congestion to the contralateral inferotemporal vortex veins (See [Video 1](#)). **F**, Ultrawidefield ICGA shows dilatation of vortex veins predominantly in the inferotemporal quadrant as compared with the superotemporal quadrant.

extrafoveal choroidal thickening at sites of macular neovascularization can show normal CCT values.²⁰ We diagnosed CSC if all of the following criteria were met. (1) Pachychoroid was accompanied by serous retinal detachment. (2) FA showed dye leakage within the serous retinal detachment. (3) Macular neovascularization was ruled out by FA, ICGA, and OCTA imaging findings. Pachychoroid neovasculopathy was diagnosed whenever macular neovascularization associated with pachychoroid was imaged by FA, ICGA, and/or OCTA. Macular neovascularization findings on OCTA were detected in the slab from the outer retina to the choriocapillaris. The presence of polypoidal lesions was evaluated on ICGA and B-mode OCT images, i.e., polyp-like choroidal vessel dilatation on ICGA and sharply peaked retinal pigment epithelium detachment on B-mode OCT. In this study, PNV meant PNV without polypoidal lesions, whereas PCV meant PNV with polypoidal lesions.

We evaluated whether retrograde pulsatile vortex venous flow was present in the early phase of video-ICGA. Moreover, we assessed whether anastomosis was present between the superotemporal and inferotemporal vortex veins and determined the dominant site of dilated temporal vortex veins on the en face OCT and ICGA images. These findings were judged by 2 experienced retinal specialists (H. Matsumoto and J. Hoshino) working collaboratively. Central choroidal thickness was measured on B-mode images employing the computer-based caliper measurement tool included in the OCT system. Central choroidal thickness was

defined as the distance between Bruch's membrane and the margin of the choroid and sclera under the fovea. Data are presented as the average \pm standard deviation.

Results

The early phase of video-ICGA showed pulsatile vortex venous flow in some of the vortex veins in 199 eyes (28.9%) of 198 patients among the 689 eyes of 681 patients with pachychoroid spectrum diseases. We next identified 22 eyes (3.2%) of 22 patients showing retrograde pulsatile vortex venous flow in the temporal vortex veins. The subjects included 5, 11, and 6 eyes with CSC, PNV, and PCV, respectively. There were 20 male and 2 female patients. Their average age was 71.4 ± 9.8 years. The average CCT was 285 ± 83 μm . En face OCT and ICGA showed inter-vortex venous anastomoses between the superotemporal and inferotemporal vortex veins in all 22 eyes. In 9 eyes, the retrograde pulsatile flow was detected in the superotemporal vortex veins, which connected to the inferotemporal vortex veins via intervortex venous anastomoses. Among these cases, contralateral inferotemporal vortex vein dilatation was dominant in 7 eyes (77.8%), whereas superotemporal

and inferotemporal vortex veins were symmetrically dilated in the other 2 eyes (22.2%). On the other hand, in 13 eyes, the retrograde pulsatile flow was detected in the inferotemporal vortex veins, which were linked to the superotemporal vortex veins via intervortex venous anastomoses. In these eyes, contralateral superotemporal vortex vein dilatation was dominant in 10 eyes (76.9%). Superotemporal and inferotemporal vortex veins were symmetrically dilated in 2 eyes (15.4%), whereas mainly inferotemporal vortex veins were dilated in 1 eye (7.7%). The demographic and clinical characteristics of these patients with pachychoroid spectrum diseases showing retrograde pulsatile vortex

venous flow are listed in [Table 1](#). Representative cases are shown in [Figures 1 to 3](#) as well as [Videos 1 to 3](#).

Discussion

Among 689 consecutive eyes diagnosed as having pachychoroid spectrum diseases, we used the early phase of video-ICGA to identify 22 eyes (3.2%) exhibiting retrograde pulsatile vortex venous flow in the temporal vortex veins. In all of these eyes, vortex venous blood flowed from the vortex veins showing retrograde pulsatile flow into the

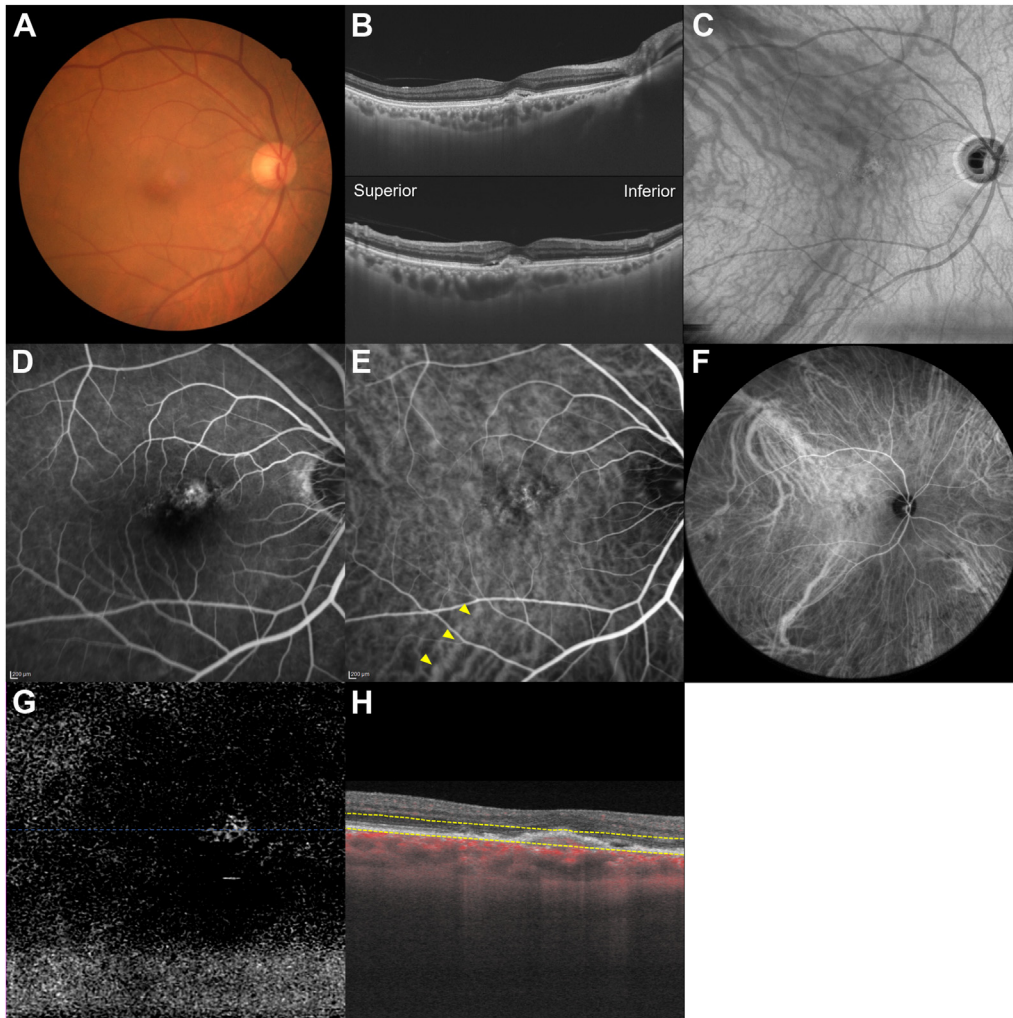


Figure 2. Images of the right eye of an 80-year-old man with pachychoroid neovascularopathy. Best-corrected visual acuity was 0.10 logarithm of the minimum angle of resolution unit. **A**, Color fundus photograph shows a retinal pigment epithelium (RPE) abnormality superonasal to the fovea. **B**, Twelve-millimeter horizontal and vertical B-mode OCT images through the fovea show pachychoroid with dilated outer choroidal vessels (vortex veins). A shallow irregular RPE detachment accompanied by subretinal fluid is present at the fovea. The central choroidal thickness is 304 μm . **C**, En face OCT image (12 mm \times 12 mm) of the choroid shows dilated vortex veins. The horizontal watershed is lost due to anastomoses between the superotemporal and inferotemporal vortex veins. Superotemporal vortex veins are more dilated than inferotemporal vortex veins. **D**, Fluorescein angiography shows window defects and mild leakage in the macular area. **E**, Indocyanine green angiography (ICGA) shows suspected macular neovascularization at the macular area. Retrograde pulsatile flow can be seen in the inferotemporal vortex veins (arrowheads). Venous blood flows from inferotemporal vortex veins affected by primary congestion to the contralateral superotemporal vortex veins (See [Video 2](#)). **F**, Widefield ICGA shows dilatation of vortex veins predominantly in the superotemporal quadrant as compared to the inferotemporal quadrant. **G**, **H**, OCT angiography (3 mm \times 3 mm) shows a network of vessels comprising type 1 macular neovascularization between the detached RPE and Bruch's membrane.

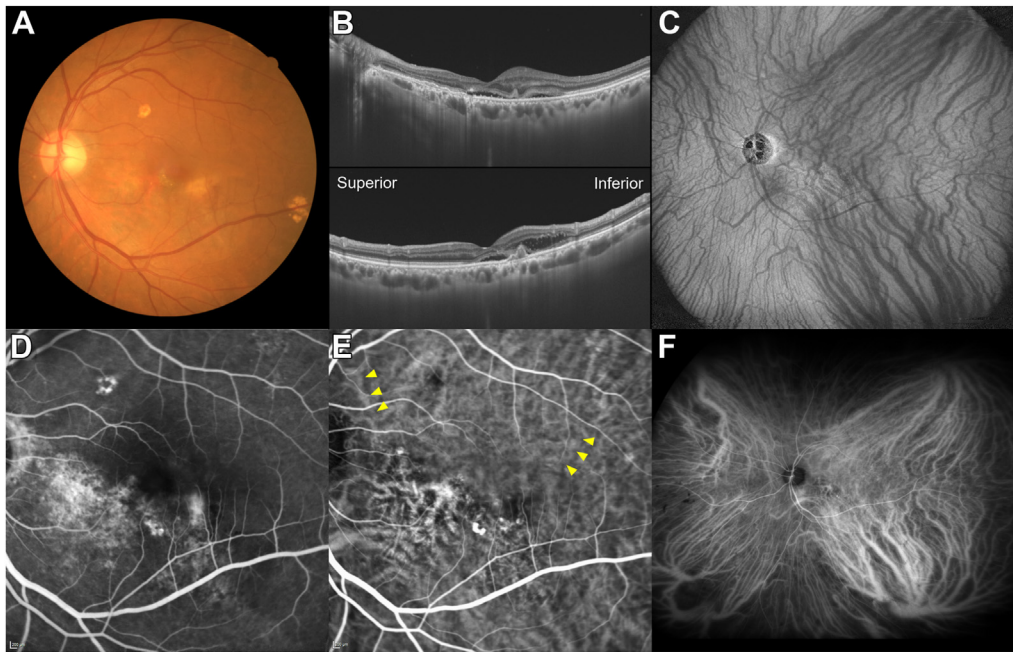


Figure 3. Images of the left eye of a 73-year-old man with polypoidal choroidal vasculopathy. Best-corrected visual acuity was 0.10 logarithm of the minimum angle of resolution unit. **A**, Color fundus photograph shows retinal pigment epithelium (RPE) degeneration accompanied by mild subretinal hemorrhage in the inferior macular area. **B**, Twelve-millimeter horizontal and vertical B-mode OCT images through the fovea show pachychoroid with dilated outer choroidal vessels (vortex veins). Vertical B-mode OCT image shows the double layer sign reflecting a branching neovascular network and sharply peaked RPE detachment due to the polypoidal lesion, which is accompanied by subretinal and intraretinal fluid. The central choroidal thickness is 280 μm . **C**, En face OCT image (20 mm \times 23 mm) of the choroid shows dilated vortex veins. The horizontal watershed has been lost due to anastomoses between the superotemporal and inferotemporal vortex veins. Inferotemporal vortex veins are more dilated than superotemporal vortex veins. **D**, Fluorescein angiography shows window defects and mild leakage in the inferior macular area. **E**, Indocyanine green angiography (ICGA) shows network vessels of macular neovascularization accompanied by polypoidal lesions in the inferior macular area. Retrograde pulsatile flow can be seen in the superotemporal vortex veins (arrowheads). Venous blood flows from superotemporal vortex veins affected by primary congestion to the contralateral inferotemporal vortex veins (See Video 3). **F**, Ultrawidefield ICGA shows dilatation of vortex veins predominantly in the inferotemporal quadrant as compared to the superotemporal quadrant.

contralateral vortex veins via intervortex venous anastomoses between the superotemporal and inferotemporal vortex veins. Furthermore, in 17 eyes (77.3%), the contralateral vortex veins were apparently dilated as compared with the primary congested vortex veins with retrograde pulsatile flow.

Prior studies using video-ICGA have demonstrated pulsatile vortex venous flow in pachychoroid spectrum diseases.^{15,18} Due to the high velocity of blood flow in the choroid,²¹ video-ICGA does not routinely detect the pulsatile flow in vortex veins. However, when congestion occurs in these veins, blood flow velocity may decrease, thereby producing the pulsatile flow observed in the vortex veins. We can reasonably assume that if the outflow disturbance impacting vortex veins is relatively mild, anterograde pulsation will be seen, and as the outflow disturbance becomes more severe, back and forth pulsation and then retrograde pulsation will become detectable. For the current study, we analyzed only cases showing obvious retrograde vortex venous flow, i.e., relatively severe outflow obstruction of at least a portion of the vortex veins.

Takahashi and Kishi described remodeling of choroidal venous drainage after vortex vein occlusion following

scleral buckling for retinal detachment.²² They identified a compensatory mechanism allowing the vortex veins with impaired outflow due to scleral buckling to form anastomotic vessels involving the vortex veins without outflow obstruction, thereby draining the congested vortex venous blood out of the eye. In their patient series, vortex veins that had been spared from the obstruction were more dilated than those with impaired outflow. Moreover, they noted that retrograde blood flow was observed in the vortex veins with impaired outflow in some of their patients.

Our monkey model of vortex vein congestion showed dilatation of supratemporal and inferotemporal vortex veins soon after these vessels had been ligated outside the sclera.¹⁶ Subsequently, however, anastomotic vessels between the temporal and nasal vortex veins developed, resulting in thinning of the temporal vortex veins and dilatation of the nasal vortex veins as compared with baseline. We speculated that venous blood that had become congested in the temporal vortex veins, as a result of the outflow obstruction, might flow into the nasal vortex veins via intervortex venous anastomoses. This would lead to nasal vortex vein dilatation.

These findings are highly consistent with our current results, including retrograde vortex venous flow, intervortex venous anastomosis, and dilated contralateral vortex veins. Therefore, we suggest that the compensatory mechanism might be functioning to relieve vortex vein congestion in pachychoroid spectrum diseases with retrograde pulsatile vortex venous flow. The primary congested vortex veins might show retrograde pulsatile flow due to severely impaired outflow, and the congested venous blood flowing into the contralateral vortex veins via intervortex venous anastomoses would then cause secondary overload of the contralateral vortex veins. Therefore, the secondarily overloaded vortex veins would presumably become more dilated than the primary congested vortex veins. The dilated vortex veins seen in pachychoroid spectrum diseases can be either primary congested vortex veins or secondarily overloaded vortex veins. Evaluating the direction of blood flow in the vortex veins may facilitate distinguishing them.

The limitations of our study include its retrospective nature, the single-center design, and small number of eyes showing retrograde pulsatile vortex venous flow on video-ICGA. Nearly all of the subjects were Japanese, such that the results may not be generalizable to pachychoroid spectrum diseases in other ethnic and/or racial groups. Moreover, we judged retrograde pulsatile vortex venous flow, asymmetric dilatation of vortex veins, and intervortex venous anastomosis subjectively.

In conclusion, in pachychoroid spectrum diseases, there are cases with severe obstruction of vortex vein outflow wherein congested venous blood appears to drain into the contralateral vortex veins via intervortex venous anastomoses, resulting in compensatory dilatation of the contralateral vortex veins. Due to this remodeling of the venous drainage route, inversion of asymmetric vortex vein dilatation might develop in pachychoroid spectrum diseases.

Footnotes and Disclosures

Originally received: January 6, 2024.

Final revision: February 23, 2024.

Accepted: March 8, 2024.

Available online: March 15, 2024. Manuscript no. XOPS-D-24-00006.

Department of Ophthalmology, Gunma University Graduate School of Medicine, Maebashi, Japan.

Disclosure(s):

All authors have completed and submitted the ICMJE disclosures form.

The author(s) have made the following disclosure(s):

H.M.: Payment or honoraria for lectures, presentations, speakers bureaus, manuscript writing or educational events—Novartis, Bayer, Chugai, Santen, and Senju.

J.H.: Payment or honoraria for lectures, presentations, speakers bureaus, manuscript writing or educational events—Novartis, Chugai, and Senju.

H.A.: Payment or honoraria for lectures, presentations, speakers bureaus, manuscript writing or educational events—Novartis, Chugai, Bayer, Senju, Santen, Otsuka, Eisai, AMO, Pfizer, Wakamoto, and Kowa.

HUMAN SUBJECTS: Human subjects were included in this study. This study, which complied with the guidelines of the Declaration of Helsinki, was performed with approval from the Institutional Review Board of Gunma University Hospital. Opt-out informed consent protocol was used for this study.

No animal subjects were included in this study.

Author Contributions:

Conception and design: Matsumoto, Kishi, Akiyama

Data collection: Matsumoto, Hoshino, Nakamura

Analysis and interpretation: Matsumoto, Kishi, Hoshino

Obtained funding: Not applicable

Overall responsibility: Matsumoto

Abbreviations and Acronyms:

CCT = central choroidal thickness; **CSC** = central serous chorioretinopathy; **FA** = fluorescein angiography; **ICGA** = indocyanine green angiography; **OCTA** = OCT angiography; **PCV** = polypoidal choroidal vasculopathy; **PNV** = pachychoroid neovascularopathy.

Keywords:

Asymmetric vortex vein dilatation, Choroidal congestion, Choroidal venous overload, Intervortex venous anastomosis, Pachychoroid.

Correspondence:

Hidetaka Matsumoto, MD, PhD, Department of Ophthalmology, Gunma University Graduate School of Medicine, 3-39-15 Showa-machi, Maebashi, Gunma 371-8511, Japan. E-mail: hide-m@gunma-u.ac.jp.

References

- Warrow DJ, Hoang QV, Freund KB. Pachychoroid pigment epitheliopathy. *Retina*. 2013;33:1659–1672.
- Cheung CMG, Lee WK, Koizumi H, et al. Pachychoroid disease. *Eye (Lond)*. 2019;33:14–33.
- Yanagi Y. Pachychoroid disease: a new perspective on exudative maculopathy. *Jpn J Ophthalmol*. 2020;64:323–337.
- Hosoda Y, Miyake M, Yamashiro K, et al. Deep phenotype unsupervised machine learning revealed the significance of pachychoroid features in etiology and visual prognosis of age-related macular degeneration. *Sci Rep*. 2020;10:18423.
- Matsumoto H, Hoshino J, Mukai R, et al. Clinical characteristics and pachychoroid incidence in Japanese patients with neovascular age-related macular degeneration. *Sci Rep*. 2022;12:4492.
- Kishi S, Matsumoto H. A new insight into pachychoroid diseases: remodeling of choroidal vasculature. *Graefes Arch Clin Exp Ophthalmol*. 2022;260:3405–3417.
- Spaide RF, Gemmy Cheung CM, Matsumoto H, et al. Venous overload choroidopathy: a hypothetical framework for central serous chorioretinopathy and allied disorders. *Prog Retin Eye Res*. 2022;86:100973.

8. Pang CE, Shah VP, Sarraf D, Freund KB. Ultra-widefield imaging with autofluorescence and indocyanine green angiography in central serous chorioretinopathy. *Am J Ophthalmol.* 2014;158:362–371 e2.
9. Hiroe T, Kishi S. Dilatation of asymmetric vortex vein in central serous chorioretinopathy. *Ophthalmol Retina.* 2018;2:152–161.
10. Kishi S, Matsumoto H, Sonoda S, et al. Geographic filling delay of the choriocapillaris in the region of dilated asymmetric vortex veins in central serous chorioretinopathy. *PLoS One.* 2018;13:e0206646.
11. Matsumoto H, Hoshino J, Mukai R, et al. Chronic choriocapillaris ischemia in dilated vortex vein region in pachychoroid neovascularopathy. *Sci Rep.* 2021;11:16274.
12. Matsumoto H, Kishi S, Mukai R, Akiyama H. Remodeling of macular vortex veins in pachychoroid neovascularopathy. *Sci Rep.* 2019;9:14689.
13. Matsumoto H, Hoshino J, Mukai R, et al. Vortex vein anastomosis at the watershed in pachychoroid spectrum diseases. *Ophthalmol Retina.* 2020;4:938–945.
14. Matsumoto H, Hoshino J, Arai Y, et al. Quantitative measures of vortex veins in the posterior pole in eyes with pachychoroid spectrum diseases. *Sci Rep.* 2020;10:19505.
15. Matsumoto H, Hoshino J, Mukai R, et al. Pulsation of anastomotic vortex veins in pachychoroid spectrum diseases. *Sci Rep.* 2021;11:14942.
16. Matsumoto H, Mukai R, Saito K, et al. Vortex vein congestion in the monkey eye: a possible animal model of pachychoroid. *PLoS One.* 2022;17:e0274137.
17. Spaide RF. CHOROIDAL BLOOD FLOW: review and potential explanation for the choroidal venous anatomy including the vortex vein system. *Retina.* 2020;40:1851–1864.
18. Gemmy Cheung CM, Teo KYC, Spaide RF. Pulsatile filling of dilated choroidal vessels in macular watershed zones. *Retina.* 2021;41:2370–2377.
19. Ikuno Y, Kawaguchi K, Nouchi T, Yasuno Y. Choroidal thickness in healthy Japanese subjects. *Invest Ophthalmol Vis Sci.* 2010;51:2173–2176.
20. Lee WK, Baek J, Dansingani KK, et al. Choroidal morphology in eyes with polypoidal choroidal vasculopathy and normal or subnormal subfoveal choroidal thickness. *Retina.* 2016;36:S73–S82.
21. Alm A, Bill A, Young FA. The effects of pilocarpine and neostigmine on the blood flow through the anterior uvea in monkeys. A study with radioactively labelled microspheres. *Exp Eye Res.* 1973;15:31–36.
22. Takahashi K, Kishi S. Remodeling of choroidal venous drainage after vortex vein occlusion following scleral buckling for retinal detachment. *Am J Ophthalmol.* 2000;129:191–198.